JOURNAL OF NEUROCHEMISTRY | 2008 | 104 | 1415–1429 doi: 10.1111/j.1471-4159.2007.05098.x

Neuronal activity enhances aryl hydrocarbon receptor-mediated gene expression and dioxin neurotoxicity in cortical neurons

Chun-Hua Lin,*,† Shu-Hui Juan,†,‡,[1] Chen Yu Wang,†,§,[1] Yu-Yo Sun,*,†,[1] Chih-Ming Chou,‡,¶ Shwu-Fen Chang,** Ssu-Yao Hu,*,† Wen-Sen Lee*,†,‡ and Yi-Hsuan Lee†,‡,§

*Division of Cell Physiology and Neuroscience, Graduate Institute of Medical Sciences, College of Medicine, Taipei Medical University, Taipei, Taiwan

†Department of Physiology, School of Medicine, College of Medicine, Taipei Medical University, Taipei, Taiwan

‡Graduate Institute of Neuroscience, College of Medicine, Taipei Medical University, Taipei, Taiwan

§Topnotch Stroke Research Center, Taipei Medical University, Taipei, Taiwan

¶Department of Biochemistry, School of Medicine, College of Medicine, Taipei Medical University, Taipei, Taiwan

**Graduate Institute of Cell and Molecular Biology, College of Medicine, Taipei Medical University, Taipei, Taiwan

Abstract

The aryl hydrocarbon receptor (AhR) is a ligand-activated transcription factor activated by dioxin and polyaromatic hydrocarbons. Recent studies have revealed that AhR activity in central neurons depends on the NMDA receptor. In this study, we investigated how the neuronal activity influence AhR-mediated dioxin-responsive gene expression and neurotoxicity. Our results show that activation of AhR by the selective agonist 2,3,7,8-tetrachlorodibenzo-*p*-dioxin induced dioxin-responsive gene expression and calcium entry, which were attenuated by AhR small interfering RNA, the NMDA receptor channel blocker MK801, and the action potential blocker tetrodotoxin (TTX). In addition, AhR-mediated gene expression was enhanced in neurons during synaptogenesis (10 days *in vitro*) compared with younger neurons (4 days *in vitro*), as was sensitivity to TTX and MK801. Furthermore, TTX and MK801 differentially affected the association of AhR and its transcriptional co-activator cAMP-responsive-element binding protein with the cytochrome P450 1A1 (cyp1A1) gene enhancer. Calcium/calmodulin-dependent protein kinase IV, the cAMP-responsive-element binding protein activating enzyme, was also activated by 2,3,7,8-tetrachlorodibenzo-*p*-dioxin in an activity-dependent manner. Finally, we found that neuronal susceptibility to dioxin insult was also maturation and activity-dependent. Together, the results suggest that neuronal activity may facilitate AhR-mediated calcium signaling, which in turn enhances AhR-mediated gene regulation and mediated maturation-dependent dioxin neurotoxicity.

Keywords: aryl hydrocarbon receptor, calcium/calmodulin-dependent protein kinase IV, CREB binding protein, neuronal activity, neuronal survival, NMDA receptor.

J. Neurochem. (2008) **104**, 1415–1429.

The aryl hydrocarbon receptor (AhR) is a ligand-activated transcription factor that belongs to the basic helix-loop-helix/Per-Arnt-Sim transcription factor superfamily (reviewed by Rowlands and Gustafsson 1997; Hahn 1998). The exogenous ligands of AhR are mainly environmental organic pollutants, including polyaromatic hydrocarbons, polychlorinated biphenyls, and dioxins (reviewed by Bock and Kohle

Received August 27, 2007; revised manuscript received October 8, 2007; accepted October 15, 2007.

Address correspondence and reprint requests to Yi-Hsuan Lee, PhD, Department of Physiology, Taipei Medical University, 250 Wu-Hsing Street, Taipei 110, Taiwan. E-mail: hsuan@tmu.edu.tw

[1]S.-H. Juan, C. Y. Wang, and Y.-Y. Sun contributed equally to this work.

Abbreviations used: $[Ca^{2+}]_i$, intracellular calcium concentration; AhR, aryl hydrocarbon receptor; ARNT, aryl hydrocarbon receptor nuclear translocator; BME, basal medium Eagles; CaMK, calcium/calmodulin-dependent protein kinase; CBP, cAMP-responsive-element binding protein; ChIP, chromatin immunoprecipitation; CYP1A1, cytochrome P450 1A1; DCF, 2,7-dichlorodihydrofluorescein; DIV, days *in vitro*; DRE, dioxin-responsive elements; FBS, fetal bovine serum; fura-2AM, fura-2 acetoxymethyl ester; GAPDH, glyceraldehyde-3-phosphate dehydrogenase; LDH, lactate dehydrogenase; MTT, 3-(4,5-dimethylthiazol-2-yl)-2,5-diphenyltetrazolium bromide; NMDA-R, NMDA receptor; PBS, phosphate-buffered saline; ROS, reactive oxygen species; SD, Sprague–Dawley; siAhR, AhR small interfering RNA; siRNA, small interfering RNA; TCDD, 2,3,7,8-tetrachlorodibenzo-*p*-dioxin; TTX, tetrodotoxin.

2006). The ligand-activated AhR translocates into the nucleus, dimerizes with the aryl hydrocarbon receptor nuclear translocator (ARNT), and binds to dioxin-responsive elements (DREs) on the target gene enhancer, thereby activating gene expression (Ma 2001). The most notable gene family activated by AhR/ARNT is the cytochrome P450 (CYP) family. One family member, CYP1A1, exerts xenobiotic metabolism for detoxification (reviewed by Mimura and Fujii-Kuriyama 2003). The xenobiotic metabolism of 2,3,7,8-tetrachlorodibenzo-*p*-dioxin (TCDD), the most potent AhR agonist as well as an environmental toxin, gives rise to metabolites that induce the production of reactive oxygen species (ROS), cytotoxicity, and carcinogenicity (Shimada and Fujii-Kuriyama 2004; Knerr and Schrenk 2006). AhR and its target genes are widely expressed in multiple brain regions including the cortex, cerebellum, and hippocampus (Hays *et al.* 2002; Williamson *et al.* 2005). Epidemiological studies revealed that TCDD preferentially impairs brain function in highly plastic neuronal populations, such as in developing brains and in brain regions involving learning and memory (Seegal, 1996; Patandin *et al.* 1999; Schantz *et al.* 2001; Powers *et al.* 2005). Recently, growing evidence on gestational and lactational dioxin exposure-induced cortical dysfunctions such as delayed active avoidance learning, reduced locomotor activity, reduced neuronal response to sensory stimuli in the sensory cortex, etc. were reported in animal model studies (Hood *et al.* 2006; Nishijo *et al.* 2007). However, the relationship between neuronal plasticity and dioxin neurotoxicity remains unclear.

Dioxin and other AhR agonists rapidly elevate the intracellular calcium concentration ($[Ca^{2+}]_i$) in both neural and non-neural cells (Hanneman *et al.* 1996; Wong *et al.* 1997; Kim and Yang 2005; Zhao *et al.* 2005; Dale and Eltom 2006). Recent studies show that AhR agonist-induced CYP1A1 expression is calcium-dependent (Le Ferrec *et al.* 2002; Dale and Eltom 2006). Furthermore, blocking the NMDA glutamate receptor (NMDA-R), the major mediator for synaptic plasticity and neuronal activity (Duguid and Sjostrom 2006; Rao and Finkbeiner 2007), abolishes TCDD-induced calcium influx and ROS production in cerebellar granular neurons (Kim and Yang 2005). This evidence suggests that AhR activation might depend upon neuronal activity. The cAMP-responsive-element binding protein (CBP) is known to affect calcium-dependent gene expression relating to neuronal plasticity (Hu *et al.* 1999; Beischlag *et al.* 2002; Impey *et al.* 2002). CBP is also one of the transcriptional co-activators for AhR (Kobayashi *et al.* 1997; Beischlag *et al.* 2002). CBP can be phosphorylated and activated by calcium/calmodulin-dependent protein kinase IV (CaMK-IV) (Impey *et al.* 2002), a protein kinase that is activated by calcium influx through the NMDA-R and the L-type voltage-gated calcium channel (Hardingham *et al.* 1999; Marshall *et al.* 2003). Therefore, it is likely that neuronal activity is involved in AhR transactivation via CaMK-IV/CBP signaling.

Although the transcriptional machinery involved in AhR-mediated gene expression is known, information regarding the regulatory mechanism of AhR activity in central neurons is still limited. Based upon the above information, we hypothesize that AhR activity might be associated with activity-dependent neuronal development. In the present study, we investigated how synaptic activity during development affects AhR-mediated gene regulation and neuronal survival. Our results show that dioxin-induced AhR activity and transactivation of downstream target genes were activity-dependent and maturation dependent in cultured neurons. Only in neurons undergoing synaptogenesis were the dioxin-induced effects sensitive to neuronal activity blockers. We further found that activity-dependent CaMK-IV/CBP signaling was involved in the activation of AhR. Lastly, we investigated the involvement of activity-dependent AhR transactivation in the susceptibility of neurons to dioxin during synaptic maturation.

Materials and methods

Materials

2,3,7,8-Tetrachlorodibenzo-*p*-dioxin was obtained from Accustandard (New Haven, CT, USA). MK801, tetrodotoxin (TTX), L-glutamate, and ellipticine were obtained from Sigma-Aldrich (St Louis, MO, USA). KN-93 was obtained from Tocris (Bristol, UK). Fura-2 acetoxymethyl ester (fura-2AM) and Fluo-3AM were obtained from Molecular Probes (Eugene, OR, USA). All common chemicals were from Sigma (St Louis, MO, USA) unless otherwise indicated.

Animals

Pregnant female Sprague–Dawley (SD) rats and neonatal 0- to 2-day-old SD rats were used in this study for the primary culture of cortical neurons and astrocytes, respectively, and were obtained from the National Institute of Experimental Animal Research, Taipei, Taiwan. Rats were killed by an overdose of sevoflurane (Abbott, Osaka, Japan) to minimize pain or discomfort in accordance with the National Institute of Health guidelines in the US regarding the care and use of animals for experimental procedures. The procedures for killing pregnant and postnatal rats in this study were reviewed and approved by the Experimental Animal Review Committee at Taipei Medical University.

Primary culture of cortical neurons

Primary cultured cortical neurons were prepared as described previously (Lee *et al.* 2000). In brief, pregnant female SD rats at 17-day gestation were anesthetized and killed to harvest the fetal rats. Cerebral cortices of fetal rats were isolated and mechanically dissociated. The cell suspension was washed three times and centrifuged at 200 *g* for 5 min in growth medium Eagles [basal medium Eagles (BME; Life Technology, Carlsbad, CA, USA) supplemented with D-glucose (33 mmol/L final), L-glutamine (2.0 mmol/L final), and 20% heat-inactivated fetal bovine serum (FBS; Hyclone, Logan, UT, USA)]. The pellet was resuspended in growth medium Eagles at approximately 3×10^5 cells/mL, and

plated onto poly-L-lysine-coated cell culture dishes at approximately 6×10^5 cells/35 mm dish, 4×10^5 cells/20 mm circular glass coverslip in 35-mm dishes, or 1.5×10^5 cells/well of a 24-well plate. Cells were incubated for 45 min in an incubator (37°C, 99% humidity, 5% CO_2) to allow cell attachment. The culture medium was then replaced by serum-free BME for further incubation. The day of cell plating was considered 0 day *in vitro* (DIV). Cultured neurons were used at 4 or 10 DIV according to the experimental design. Cultures consisted of approximately 85–90% neurons and 10% astroglia as characterized by immunolabeling of neuronal and astrocyte markers microtubule-associated protein-2 and glial fibrillary acidic protein, respectively (Supplementary Fig. S1). Differential synaptic maturation in 4 and 10 DIV neurons was characterized by western blot analysis of a synaptic protein syntaxin 4 (Supplementary Fig. S1).

Primary culture of astrocytes

Astrocyte cultures were prepared as described previously (McCarthy and de Vellis 1980). In brief, cerebral cortices were harvested from 1- to 2-day-old SD rats, homogenized by mechanical dissociation, and the cell suspension was diluted in Dulbecco's modified Eagle's medium/F12 (Invitrogen, Carlsbad, CA, USA) supplemented with 10% heat-inactivated FBS. Cells were seeded onto 75-cm^2 flasks at an initial density of 2×10^6 cells/flask. Six to 8 days after seeding, microglia and oligodendrocytes were removed by orbital shaking of the culture flasks at 160 rpm for 24 h at 37°C. The suspended cells were decanted to obtain pure astrocytes adhered at the bottom. The purified astrocytes were subcultured in 24-well plates with Dulbecco's modified Eagle's medium/F12 medium containing 10% FBS for 24 h, and the cultured astrocytes were used for experiments when they reached 80–90% confluence.

Western blot analysis

Cultured neurons were harvested with lysis buffer, and cell lysate containing 50 μg of protein was subjected to 7.5% sodium dodecyl sulfate–polyacrylamide gel electrophoresis. Protein samples separated on the electrophoresed gel were transferred to a nitrocellulose membrane (Hybond ECL membrane; Amersham, Buckinghamshire, England), and probed with properly diluted antibodies against AhR (Biomol, Plymouth Meeting, PA, USA) and glyceraldehyde-3-phosphate dehydrogenase (GAPDH; Biogenesis, Poole, England). The blot was then probed with horseradish peroxidase-conjugated secondary antibody (Jackson ImmunoResearch Laboratories, West Grove, PA, USA) and visualized with horseradish peroxidase-reactive chemiluminescence reagent (Pierce, Rockford, IL, USA). The relative intensity of each protein band was analyzed using the Digital Science Electrophoresis Documentation and Analysis System (Berthold Technologies, Bad Wilbad, Germany).

Measurement of intracellular calcium concentration

Intracellular $[Ca^{2+}]$ was measured in cortical neurons by fluorescence spectrophotometry (Lee *et al.* 2000) and confocal fluorescent microscopy. For fluorescent spectrophotometry, cortical neurons were grown on glass coverslips until the day of the experiment, and loaded with 5 μmol/L of fura-2AM for 30 min at 37°C. At the end of the loading period, cells were washed twice with phocal buffer (125 mmol/L NaCl, 5 mmol/L KCl, 2 mmol/L $MgCl_2$, 1.8 mmol/L $CaCl_2$, and 15 mmol/L glucose; pH 7.4) and equilibrated in the incubator for another 1 h for de-esterification. The coverslip was inserted into a quartz cuvette and placed in the thermostat holder of a Hitachi F-4500 spectrofluorometer (Tokyo, Japan). Fluorescence of Ca^{2+}-bound and Ca^{2+}-free fura-2M was measured by rapidly alternating the dual excitation wavelengths between 340 and 380 nm and electronically separating the resultant fluorescence signals at an emission wavelength of 510 nm. The ratio (R) of the fluorescence at the 2 wavelengths was computed and used to calculate changes in $[Ca^{2+}]_i$. Ratios of maximum (R_{max}) and minimum (R_{min}) fluorescence of fura-2 were determined by the addition of ionomycin (10 mmol/L) in the presence of phosphate-buffered saline (PBS) containing 5 mmol/L Ca^{2+}, and by adding 5 mmol/L EGTA and 1 mmol/L $MnCl_2$ at pH 8 in Ca^{2+}-free PBS, respectively. The $[Ca^{2+}]_i$ was obtained using the following equation: $[Ca^{2+}]_i = Kd \times \beta \times (R - R_{min})/(R_{max} - R)$, in which Kd = 224 nmol/L and β = 6.9352 was assumed. For confocal microscopy of real-time $[Ca^{2+}]_i$ imaging, cells were loaded with 2 μmol/L Fluo-3AM for 30 min, followed by application of 20 nmol/L TCDD (Model FV500; Olympus, Tokyo, Japan). The captured images were analyzed using FLUOVIEW software (version 4.0, Olympus) to obtain the relative fluorescent intensity of each coverslip sample. The percentage of neurons responding to TCDD treatment was obtained by randomly selecting five microscopic fields for each group, counting the number of cells with $[Ca^{2+}]_i$-increased response, and dividing by the total cell number in the field. The data were averaged within each group.

Transfection and transcriptional activity assay

A luciferase reporter plasmid driven by a DRE activated by the AhR-ARNT complex was used for this assay. In brief, oligonucleotides with three copies of DRE (GAGTTGCGTGAGAAGAGCC) in the rat cyp1A1 enhancer region were cloned into the *Kpn*I and *Nhe*I sites of the pGL3-promoter vector (Promega, Madison, WI, USA). Sequence identities were confirmed using an ABI PRISM 377 DNA Analysis System (Wellesley, MA, USA). To assay reporter activity of the pGL3-3xDRE construct, cortical neurons were transiently transfected with 1 μg of the pGL3-3xDRE promoter *firefly* luciferase construct, and 0.1 μg of the pRL-TK *Renilla* luciferase normalization vector construct (Promega) for 5 h using Lipofectamine 2000™ reagent (Invitrogen). The DNA-transfected cells were recovered in culture medium for 24 h, then pre-treated with channel blockers or enzyme inhibitors for 5 min and 30 min, respectively, followed by the TCDD treatment for another 5 h. Treated cells were then lysed and luciferase activity was assayed using the Dual-Luciferase Assay System (Promega). The luminescence was detected and analyzed using a luminometer. The DRE-driven gene expression was calculated and represented as the ratio of firefly/*Renilla* luciferase activity. The relative luciferase activity of each sample was calculated by comparing the ratio to the mean value of the respective control group. Data were averaged within each group.

Measurement of ROS production using 2,7-dichlorodihydrofluorescein

Generation of ROS was measured using the fluorescent probe 2,7-dichlorodihydrofluorescein (DCF) diacetate as previously described (Jung *et al.* 2001). In brief, neurons were cultured in a 24-well

culture plate with approximately 1.5×10^5 cells/well. DCF-diacetate was added to each well, along with 20 nmol/L TCDD, to a final concentration of 10 μmol/L, and cells were incubated for 30 min at 37°C. After incubation, cells were washed twice and resuspended in PBS. The fluorescent intensity of the cell suspension was measured using a HIDEX Chameleon microplate reader (Turku, Finland) with an excitation wavelength at 485 nm and an emission wavelength at 530 nm. The arbitrary fluorescent units of each well in the experimental groups were divided by the mean value of the control group to obtain the relative fluorescence intensity.

Reverse-transcribed PCR

Total RNA was prepared by directly lysing the cultured neurons in extraction buffer (Trizol/phenol/chloroform), and reverse transcribing mRNAs into cDNA using oligo-dT and SuperScript™ II reverse transcriptase (Invitrogen). The cDNAs were subjected to PCR to measure the expression of CYP1A1 and the housekeeping gene GAPDH as an internal control. Primer sequences for amplification of cDNA were 5′-CTTTGGAGCTGGGTTTGACAC-3′ and 5′-CCTGCCACTGGTTCACAAAGAC-3′ (for CYP1A1); and 5′-GACCCCTTCATTGACCTCAAC-3′ and 5′-GATGACCTTGCCCACAGCCTT-3′ (for GAPDH). The PCR protocol included 30 cycles of denaturation for 1 min at 94°C, annealing for 1 min at 55–60°C, and extension for 1 min at 72°C. Reaction products were separated by electrophoresis on a 2% agarose gel. Bands were visualized and quantified using an electrophoresis image analysis system (Eastman Kodak Co., Rochester, NY, USA). Net intensity of each band was normalized by the band intensity of GAPDH and divided by the normalized intensity of the control group to obtain the ratio-to-control value.

Chromatin immunoprecipitation assay

Chromatin immunoprecipitation (ChIP) assay was performed according to the instructions of Upstate Biotechnology Inc. (Lake Placid, NY, USA) with minor modifications. Briefly, 6×10^5 cortical neurons were cultured in 35-mm dishes and incubated with 1% formaldehyde for 15 min for DNA–protein cross-linking, followed by addition of 0.05 mL of 2.5 mol/L glycine and incubation for another 5 min. Cells were washed and harvested in cold PBS. After brief centrifugation, the pellet was resuspended and homogenized in ice-cold hypotonic buffer (5 mmol/L PIPES pH 8.0, 0.5% IPGEAL CA-630, 0.5 mmol/L phenylmethylsulfonyl fluoride, and protease inhibitor cocktail), centrifuged at 15 000 *g*, and the pellet was resuspended in sonication buffer (10 mmol/L EDTA, 50 mmol/L Tris–HCl pH 8.0, 0.5 mmol/L phenylmethylsulfonyl fluoride, and protease inhibitor cocktail). Each sample was sonicated at 4°C and centrifuged at 2300 *g*, and the supernatant was subjected to immunoprecipitation overnight using the appropriate antibodies [either anti-AhR (Biomol) or anti-CBP (Santa Cruz, Santa Cruz, CA, USA) antibodies], followed by incubation with salmon sperm DNA/protein G agarose slurry (Upstate, Charlottesville, VA, USA) to immobilize the DNA–protein-antibody complex. DNA–protein complexes were then eluted with 200 μL of elution buffer (Tris-EDTA buffer containing 1% sodium dodecyl sulfate) for 30 min, and the cross-links were reversed by overnight incubation at 65°C. DNA was purified using a PCR purification kit (Qiagen, Hilden, Germany), and amplified by PCR with primers flanking the promoter of the cyp1A1 gene containing the DRE sequence (base pair −1166 to −977; Accession Number NW_047799), 5′-CCTCTCAAACCCCACCCCAACGCCCCGGGA-3′ and 5′-CCCACCTGGCTGGGGACAAGGTGCCCCGGA-3′. The PCR products were electrophoresed on a 1.2% agarose gel, and a PCR product at the expected size of 190 bp was visualized, quantified using Image analysis system (Eastman Kodak Co.), and eluted from the agarose gel for sequencing to verify the site of amplification.

Immunofluorescence double labeling of CaMK-IV and CBP

Cultured cortical neurons at 10 DIV were pre-treated with 10 μmol/L MK801 or 1 μmol/L TTX for 5 min, or with KN-93 for 30 min, followed by 20 nmol/L TCDD treatment for 10 min. The treatment was terminated by rinsing cells with Earle's Balanced Salt solution (containing 117 mmol/L NaCl, 1 mmol/L NaH_2PO_4, 5.3 mmol/L KCl, 26 mmol/L $NaHCO_3$, 0.8 mmol/L $MgSO_4$, 1.8 mmol/L $CaCl_2$, and 5.6 mmol/L D-glucose, pH 7.4), followed by incubation with fixative solution (4% formaldehyde in 20 mmol/L PBS) for 30 min at 25°C. Fixed cells were permeabilized with pre-chilled $EtOH/CH_3COOH$ (95%/5%) for 15 min at −20°C followed by sequential incubation with blocking solution, properly diluted rabbit anti-CBP polyclonal antibody (Santa Cruz, Delaware, CA, USA) at 1 : 1000, and mouse anti-CaMK-IV monoclonal antibody (BD Transduction, Oakville, ON, Canada) at 1 : 500. Immunofluorescence double labeling was performed using FITC-conjugated goat anti-rabbit IgG (Jackson ImmunoResearch Laboratories) and Texas red-conjugated goat anti-mouse IgG. (Jackson ImmunoResearch Laboratories). Fluorescent micrographs were captured by confocal laser scan microscope (Model FV500; Olympus) and digital images were merged by FLUOVIEW software. Percentage of CaMK-IV-CBP co-localization was quantified by dividing the number of CaMK-IV/CBP co-localized neurons by all the CBP-positive neurons in each randomly selected microscopic field. Data from five microscopic fields were calculated and averaged within each group.

Transfection of small interfering RNA

The small interfering RNA (siRNA) duplexes were chemically synthesized and annealed by Ambion (Austin, TX, USA). Cortical neurons were seeded onto 24-well plates and transfected with either 40 pmole AhR small interfering RNA (siAhR) (5′-GCUGGACAAACUCUCCGUUTT-3′, targeted exon: XM_579375: exon 2; 5′-GCAUUUUAAAUGAAGCCUATT-3′, targeted exon(s): XM_579375: exon 11; Ambion) or scrambled control RNA (Ambion) in 200 μL of Lipofectamine™ 2000 (Invitrogen) for 5 h. The transfection mixture was then replaced with fresh BME medium and cells were incubated for an additional 72 h to achieve significant knockdown of AhR expression. The knockdown efficiency of siAhR was analyzed by western blot analysis and RT-PCR to measure the protein and mRNA levels of AhR, respectively. AhR activity was measured by DRE-driven luciferase activity assay.

Neuronal survival analysis

The survival rate of cultured neurons was measured using the 3-(4,5-dimethylthiazol-2-yl)-2,5-diphenyltetrazolium bromide (MTT) reduction activity assay for cell viability and the lactate dehydrogenase (LDH) release assay for cell damage (Lee *et al.* 2000). For the MTT assay, TCDD-treated cells were incubated with MTT for 4 h, followed by addition of 0.3 mL of 0.4 N HCl in

isopropanol to the mixture overnight to dissolve the formazan. The dissolved suspension was subjected to an ELISA reader and the absorbance at a wavelength of 600 nm ($A_{600\ nm}$) was measured. For the LDH release assay, TCDD-treated cells were equilibrated with BME medium for 1 h, and 250 μL of culture medium was collected and incubated with 0.1 mg of β-NADH in 1.2 mL of 0.1 mol/L phosphate buffer for 5–15 min at 25°C. The absorbance at a wavelength of 340 nm was measured for 3 min immediately after 0.1 mol/L sodium pyruvate was added to the mixture. The unit activity of LDH was calculated by multiplying the decrease of A_{340} in 1 min by 4000 to obtain the activity in 1 mL of sample.

Statistical analysis

Statistical analysis was performed using GraphPad Prism® 4 software (GraphPad Software, San Diego, CA, USA). Data were expressed as mean ± SEM. Statistical analysis was performed using the non-parametric one-way ANOVA followed by the Bonferroni multiple comparison *post hoc* test or an unpaired Student's *t*-test to compare designated pairs of groups. A paired Student's *t*-test was used to evaluate changes in $[Ca^{2+}]_i$ before and after TCDD treatment. Statistic significance was assumed if $*p < 0.05$.

Results

Blockade of neuronal activity reduces TCDD-induced AhR activities

In order to study the involvement of neuronal activity in dioxin activation of AhR in central neurons, we first asked whether blockade of neuronal activity could affect the TCDD-induced $[Ca^{2+}]_i$ influx, dioxin-responsive gene expression, and ROS production. We addressed this question by blocking action potentials and NMDA-R activity in the TCDD-treated cultured neurons using the voltage-gated sodium channel blocker TTX and the NMDA-R channel blocker MK801, respectively. The cultured neurons used in this study were 10 DIV cortical neurons undergoing synaptic maturation (Weiss *et al.* 1986; Chang and Reynolds 2006) that express synaptic protein syntaxin 4 (Supplementary Fig. S1b). The concentration of TCDD used in this experiment was 20 nmol/L, which has been reported by others to induce ROS production in neurons (Kim and Yang 2005). Our results show that both 1 μmol/L TTX and 10 μmol/L MK801 completely blocked TCDD-induced increase in $[Ca^{2+}]_i$ (Fig. 1a and b), partially reduced TCDD-induced DRE-driven luciferase activity (Fig. 1c), and reversed TCDD-induced ROS production (Fig. 1d). In addition, TCDD-induced ROS formation was blocked by 500 nmol/L of ellipticine, an inhibitor of CYP1A1, implicating that TCDD may induce the expression or activity of CYP1A1 in neurons. Furthermore, we excluded the possibility that neuronal activity by itself could induce dioxin-responsive gene expression, as an increase in neuronal activity, i.e. high K^+ or glutamate treatment, in the absence of TCDD did not elevate DRE-driven luciferase activity (Fig. 1e). Together with the DRE-driven luciferase activity results, these data suggest that both synaptic activity and NMDA-R are involved in dioxin-induced AhR activity in cortical neurons.

Developmental changes of TCDD-induced AhR activity in cortical neurons are activity-dependent

Neuronal activity is important for neuronal development and is especially important for plasticity in synaptic modification and synaptic formation. Therefore, it is likely that the neuronal response to dioxin may vary during neural development. We examined this possibility by testing the TCDD-induced $[Ca^{2+}]_i$ increase and dioxin-responsive gene expression in cultured neurons at two different developmental stages, 10 DIV at synapse formation stage and 4 DIV without synaptic connections as expressed by the differential expression of syntaxin 4 (Supplementary Fig. S1b). TCDD concentrations ranging from 1 to 100 nmol/L were used to examine the dose-dependent effect. The results show that TCDD-induced elevations of $[Ca^{2+}]_i$ and DRE-driven luciferase activity in a dose-dependent manner and were much higher in 10 DIV cortical neurons than that in 4 DIV neurons (Fig. 2a and b). In addition, as our neuronal culture consists of approximately 10% of astrocytes (Supplementary Fig. S1a), we examined whether TCDD could induce a similar calcium response in a pure astrocyte culture. Figure 2b shows that the 20 nmol/L TCDD-induced calcium response was similar to the 4 DIV neurons but much less than the 10 DIV neurons. This result further suggests that the dioxin-induced responses in the 10 DIV culture may mainly come from neurons but with less from astrocytes.

If the higher AhR activity in the 10 DIV cortical neurons were due to higher synaptic activity, one would expect that these neurons would also be more sensitive to activity blockers than 4 DIV neurons. To test this hypothesis, we examined whether TTX and MK801 have differential effects on TCDD-induced $[Ca^{2+}]_i$ and the expression of CYP1A1 in 4 and 10 DIV cortical neurons. Interestingly, our results showed that 1 μmol/L TTX did not reduce TCDD-induced $[Ca^{2+}]_i$ and the expression of CYP1A1 in 4 DIV as it did in 10 DIV neurons (Fig. 2c and d). However, 10 μmol/L MK801 blocked both of these responses in both 4 and 10 DIV (Fig. 2c and e). This result suggest that NMDA-R is involved in the AhR activity throughout the neuronal development, whereas the TTX-sensitive action potential firing or synaptic transmission seems to contribute to the maturation-dependent neuronal response to dioxin.

Effects of TTX and MK801 on the association of AhR and CBP with the cyp1A1 enhancer

We further investigated the mechanism of how neuronal activity is involved in AhR-mediated gene expression. CBP is a calcium-dependent transcriptional co-activator for AhR

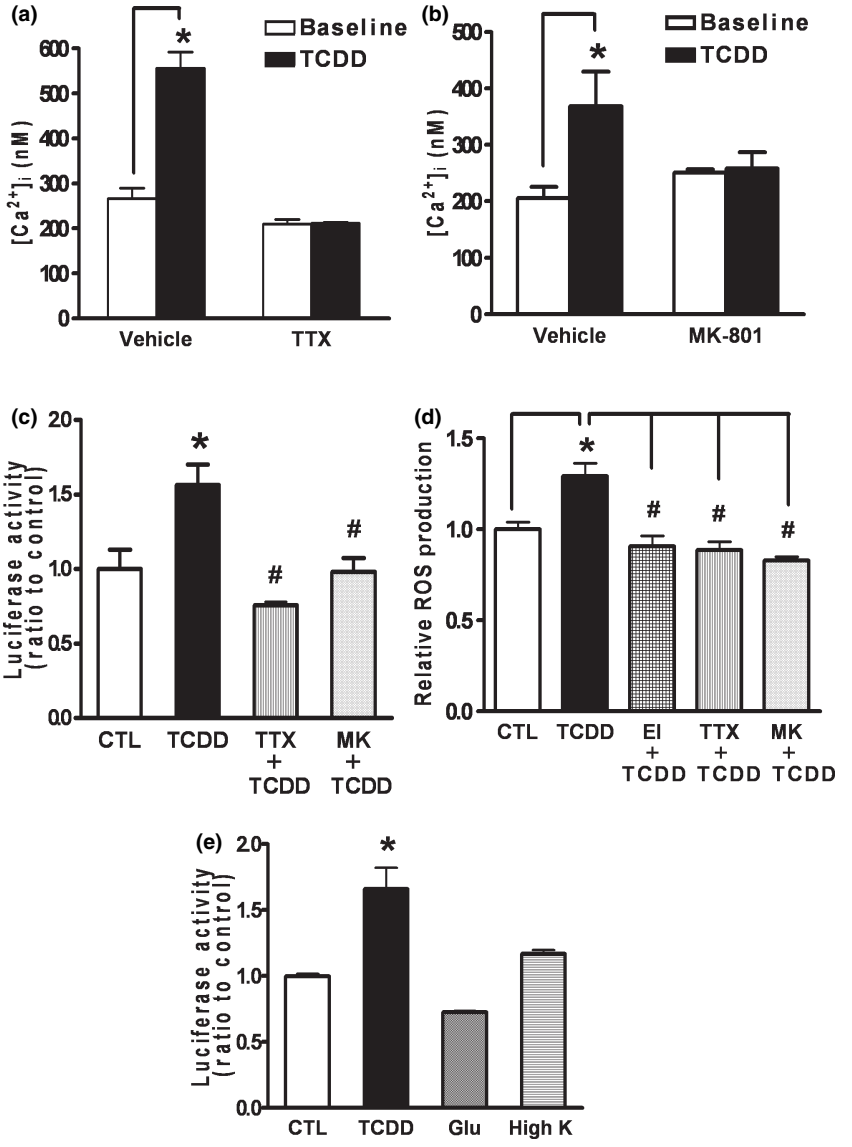

Fig. 1 TCDD-induced $[Ca^{2+}]_i$ and DRE-driven luciferase activity are sensitive to both an NMDA-R antagonist and an action potential blocker in cortical neurons. Cortical neurons at 10 DIV were subjected to $[Ca^{2+}]_i$ measurements (a and b), DRE-driven luciferase activity assay (c), and ROS formation analysis (d) in the presence or absence of 1 μmol/L TTX (a, c, and d) or 10 μmol/L MK801 (b, c, and d). For the ROS formation experiment, the cyp1A1 inhibitor ellipticine (EI) at 500 nmol/L was used as a positive control to show that the response is mediated by cyp1A1. In (e), cultured cells were treated with 100 μmol/L L-glutamate (Glu) or 30 mmol/L KCl for 5 h in the absence of TCDD for the DRE-driven luciferase activity assay. For the $[Ca^{2+}]_i$ measurements, the data represent the mean ± SEM (n = 3). *$p < 0.05$ when compared with the respective baseline level by paired t-test. For the luciferase activity assay and ROS formation, the data represent the mean ± SEM (n = 4). *$p < 0.05$ when compared with the respective CTL group by unpaired t-test, and $^{\#}p < 0.05$ when compared with the respective TCDD group by unpaired t-test.

and many other transcription factors and is highly related to synaptic plasticity. However, it is unknown whether CBP is recruited to the AhR/ARNT protein complex that binds to DNA. Therefore, we used the ChIP assay to examine if TCDD-induced association of CBP with the AhR-DNA complex by pulling down the DNA fragment of the cyp1A1 gene enhancer containing the AhR binding element using an anti-CBP antibody. Interaction of AhR with the cyp1A1 enhancer was also analyzed by ChIP assay using an anti-AhR antibody for immunoprecipitation. The immunoprecipitated cyp1A1 enhancer fragment was amplified by PCR to examine the association of AhR and CBP. Figure 3a shows that TCDD induced both AhR and CBP binding to the cyp1A1 enhancer within 1 h. We further found that TTX and MK801 differentially reduced, not only CBP, but also AhR association with the cyp1A1 enhancer. TTX reduced

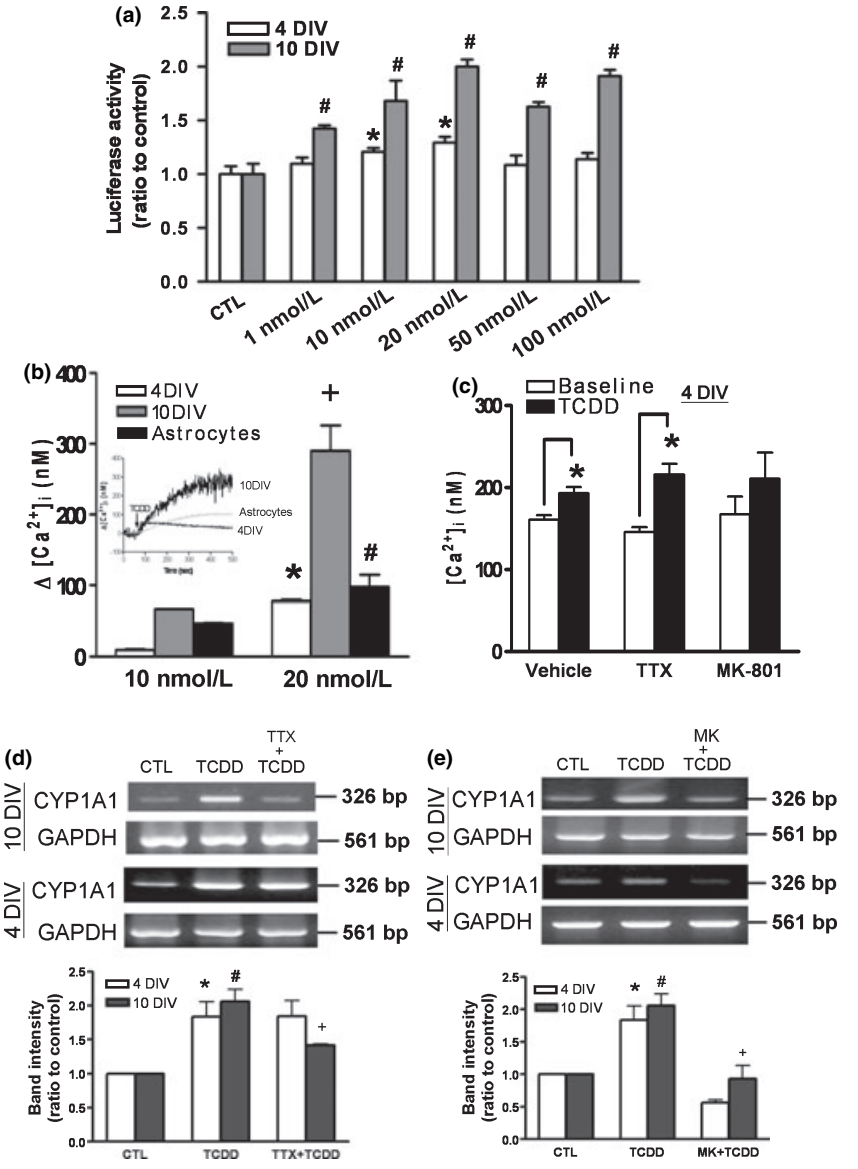

Fig. 2 Developmental changes of TCDD-induced AhR activities in cortical neurons. (a) The cortical neurons at 4 and 10 DIV were subjected to the DRE-driven luciferase activity assay in the presence of TCDD at 1, 10, 20, 50, and 100 nmol/L. Data represent the mean ± SEM of fold changes in luciferase activity relative to the control group ($n = 3$). $^{*}p < 0.05$ and $^{\#}p < 0.05$ when compared with the respective control group (CTL) by unpaired *t*-test. (b) Cultured neurons and astrocytes were treated with TCDD at 10 and 20 nmol/L and subjected to $[Ca^{2+}]_i$ measurements using fluorescent spectrophotometry. The increase of $[Ca^{2+}]_i$ ($\Delta[Ca^{2+}]_i$) was calculated by subtracting the plateau level of TCDD-increased $[Ca^{2+}]_i$ by the baseline level. (c) TCDD-induced DRE-driven luciferase activity in 4 DIV neurons. (d) Effect of TTX and MK801 on the TCDD-induced increase in $[Ca^{2+}]_i$ in 4 DIV neurons. (e) Effect of TTX and MK801 on the TCDD-induced increase in cyp1A1 mRNA in 4 and 10 DIV neurons. The concentration of TCDD used in (c, d, and e) was 20 nmol/L, and the concentration of MK801 and TTX used in (c, d, and e) were 10 and 1 μmol/L, respectively. Data represent the mean ± SEM ($n = 4$) of $\Delta[Ca^{2+}]_i$ (b and d), luciferase activity (c), and relative band intensity (e) of each group. $^{*}p < 0.05$, $^{+}p < 0.05$, and $^{\#}p < 0.05$ when compared with the 10 nmol/L TCDD-treated group in 4 and 10 DIV cortical neurons and astrocytes by one-way ANOVA analysis, respectively.

TCDD-induced AhR-associated cyp1A1 enhancer from 2.04-fold (over the control) to 0.3-fold, but only reduced CBP-associated enhancer to 1.25-fold from 1.79-fold (Fig. 3b). In contrast, MK801 completely abolished the CBP-enhancer association, but only partially reduced the AhR-enhancer interaction (Fig. 3c). Together, these results suggest that TTX-sensitive action potential firing or synaptic transmission differs from the NMDA-R activity in regulating the activity-dependent association of CBP and AhR with the cyp1A1 enhancer induced by TCDD.

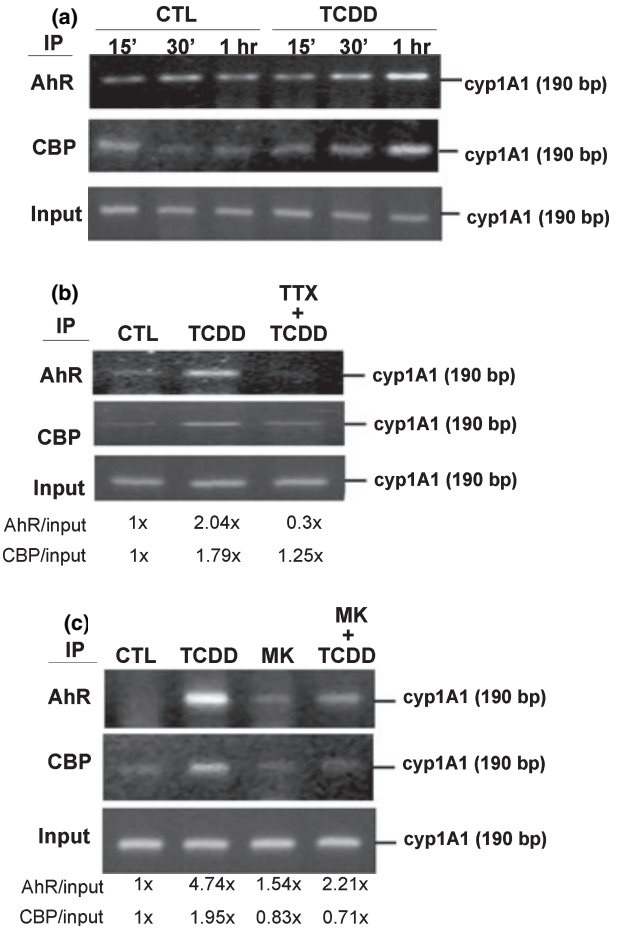

Fig. 3 Blockade of neuronal activity reduces TCDD-induced AhR and CBP association with the *cyp1A1* promoter. The neurons at 10 DIV were treated with 20 nmol/L TCDD for 15 min, 30 min, or 1 h; in (b) and (c) neurons were pre-treated with 1 μmol/L TTX and 10 μmol/L MK801 (MK) for 5 min, followed by 20 nmol/L TCDD treatment for 1 h. Cells were harvested and subjected to chromatin immunoprecipitation (ChIP) assay. The DNA associated with AhR or CBP were immunoprecipitated with anti-AhR or anti-CBP antibody, respectively, and the amount of AhR- and CBP-associated with the *cyp1A1* promoter DNA fragment of 190 bp was determined by PCR.

TCDD induces nuclear translocation of CaMK-IV, the activating enzyme of CBP

To further clarify how CBP is activated by TCDD in an activity-dependent manner, we examined whether the CBP activating enzyme CaMK-IV is activated by dioxin. We used KN-93, a pan-CaMK inhibitor, to examine its effect on TCDD-induced gene expression. Figure 4a shows that 10 μmol/L of KN-93 partially reduced TCDD-induced DRE-driven luciferase activity to a similar degree as TTX and MK801. In the ChIP assay, KN-93 abolished the association of both AhR and CBP with the cyp1A1 enhancer (Fig. 4b). To further examine if CaMK-IV is activated by TCDD, we immunolabeled CaMK-IV in cortical neurons and examined its subcellular localization following TCDD treatment using confocal fluorescent microscopy. Figure 4c shows that CaMK-IV was found primarily in the cytoplasmic compartment in the vehicle-treated group. In the TCDD-treated group, the distribution of CaMK-IV was shifted to the nucleus and co-localized with nuclear CBP. Co-localization of CaMK-IV with nuclear CBP was higher in the TCDD-treated group (33%) than in the vehicle-treated group (14%). Pre-treatment with KN-93, TTX, and MK801 significantly reduced the TCDD-induced nuclear translocation of CaMK-IV and its co-localization with CBP (Fig. 4d). These results suggest that CaMK-IV can be activated by TCDD in an activity-dependent manner and might in turn activate CBP to facilitate AhR-mediated gene expression.

Knockdown of AhR expression diminishes TCDD activation of CaMK-IV

As the activation of CaMK-IV is calcium-dependent, it is likely that the dioxin induction of $[Ca^{2+}]_i$ might contribute to CaMK-IV activation. We further ask whether AhR is required for TCDD-induced $[Ca^{2+}]_i$ and the subsequent activation of CaMK-IV. We resolved this using siAhRto knockdown AhR expression. The knockdown efficiency of siAhR in 10 DIV cortical neurons was approximately 50% as assessed by western blot analysis and RT-PCR (Fig. 5a). Figure 5b shows that dioxin-responsive gene expression was completely abolished by siAhR treatment. TCDD-induced $[Ca^{2+}]_i$ was significant in the scrambled RNA-transfected culture, and the response was reduced by siAhR (Fig. 5c). The population of neurons responsive to TCDD was reduced from 30% in the scrambled RNA-transfected culture to 10% in the siAhR-transfected culture (Fig. 5d). It is noted that the TCDD-induced calcium response in the scrambled RNA-transfected neurons was lower than the one in the non-transfected neurons as shown in Figure 2b. To clarify whether the siAhR reduction of TCDD-induced $[Ca^{2+}]_i$ was due to the changes of membrane properties by the lipofectamine treatment, we tested the depolarizing agent-evoked $[Ca^{2+}]_i$ using 20 mmol/L KCl treatment onto the transfected cultures. The result shows that both scrambled and siAhR-transfected cells well responded to the high K^+ stimulation with similar degree of $[Ca^{2+}]_i$-elevating response (Supplementary Fig. S1c). Therefore, although the TCDD-induced $[Ca^{2+}]_i$ increase in the scrambled RNA-transfected neurons was lower than the one in the non-transfected neurons (Fig. 2b), their responses to TCDD as well as to the depolarizing agent are still well preserved. Furthermore, siAhR-treated neurons had much less nuclear CaMK-IV in the nucleus after TCDD treatment when compared with the scrambled RNA-transfected group (Fig. 5e). Collectively, these results suggest that AhR is required for TCDD-induced $[Ca^{2+}]_i$ elevation and CaMK-IV activation.

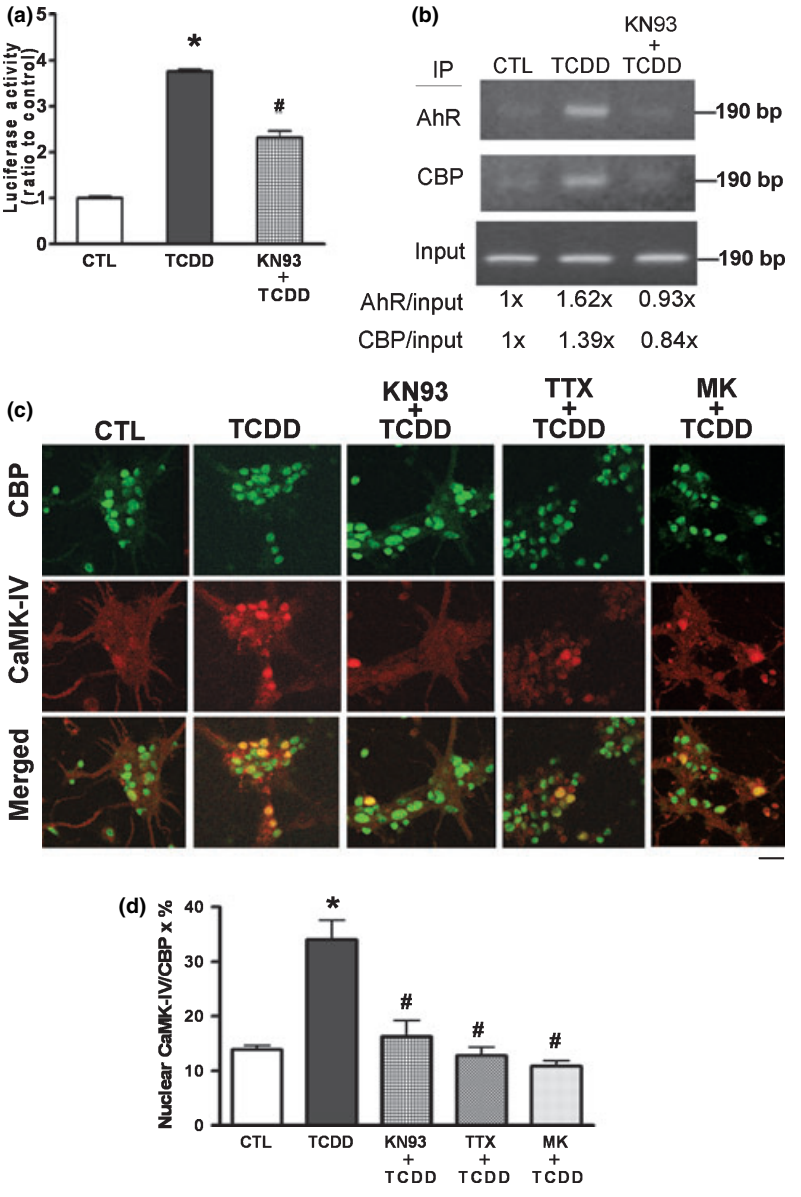

Fig. 4 TCDD induces nuclear translocation of CaMK-IV, and a CaMK inhibitor inhibits DRE-driven gene expression. (a) Cortical neurons at 10 DIV were co-transfected with pGL-3xDRE and pRL-TK constructs for 24 h, followed by pre-treatment with 10 μmol/L KN-93, and treatment with 20 nmol/L TCDD for 5 h. Cells were harvested for luciferase activity assay. Data represent the mean ± SEM ($n = 4$). *$p < 0.05$ when compared with CTL group, and #$p < 0.05$ when compared with the TCDD-treated group by unpaired *t*-test. (b) Neurons were pre-treated with vehicle (Earle's Balanced Salt solution) or 10 μmol/L KN-93, followed by 20 nmol/L TCDD stimulation for 1 h. Cells were subjected to ChIP assay for the binding of AhR or CBP to the *cyp1A1* promotor. The amount of AhR- and CBP-bound cyp1A1 promoter DNA fragment was determined by PCR. (c) Fluorescent double-labeling and confocal microscopy of CBP and CaMK-IV in 10 DIV cortical neurons upon TCDD treatment. Cells were pre-treated with 10 μmol/L KN-93 for 30 min, 1 μmol/L TTX, and 10 μmol/L MK801 for 5 min, followed by 20 nmol/L TCDD for 30 min. Dual-labeled immunofluorescence showing CBP (green by FITC) and CaMK-IV (red by Texas Red). Merged images showed co-localized structures in yellow. Data represent the mean ± SEM ($n = 4$) of percentage of CaMK-IV co-localization with CBP. *$p < 0.05$ when compared with the control group by one-way ANOVA analysis, and #$p < 0.05$ when compared with the TCDD-treated group by unpaired *t*-test. Scale bar: 25 μm.

Dioxin neurotoxicity varies depending on the developmental stage and neuronal activity

From the above results, it is likely that if AhR-mediated xenobiotic gene expression is activity-dependent, similar phenomena may regulate the effect of dioxin on neuronal survival. Therefore, we examined if neuronal survival after TCDD treatment varies at different developmental stages, and whether neuronal survival is sensitive to activity

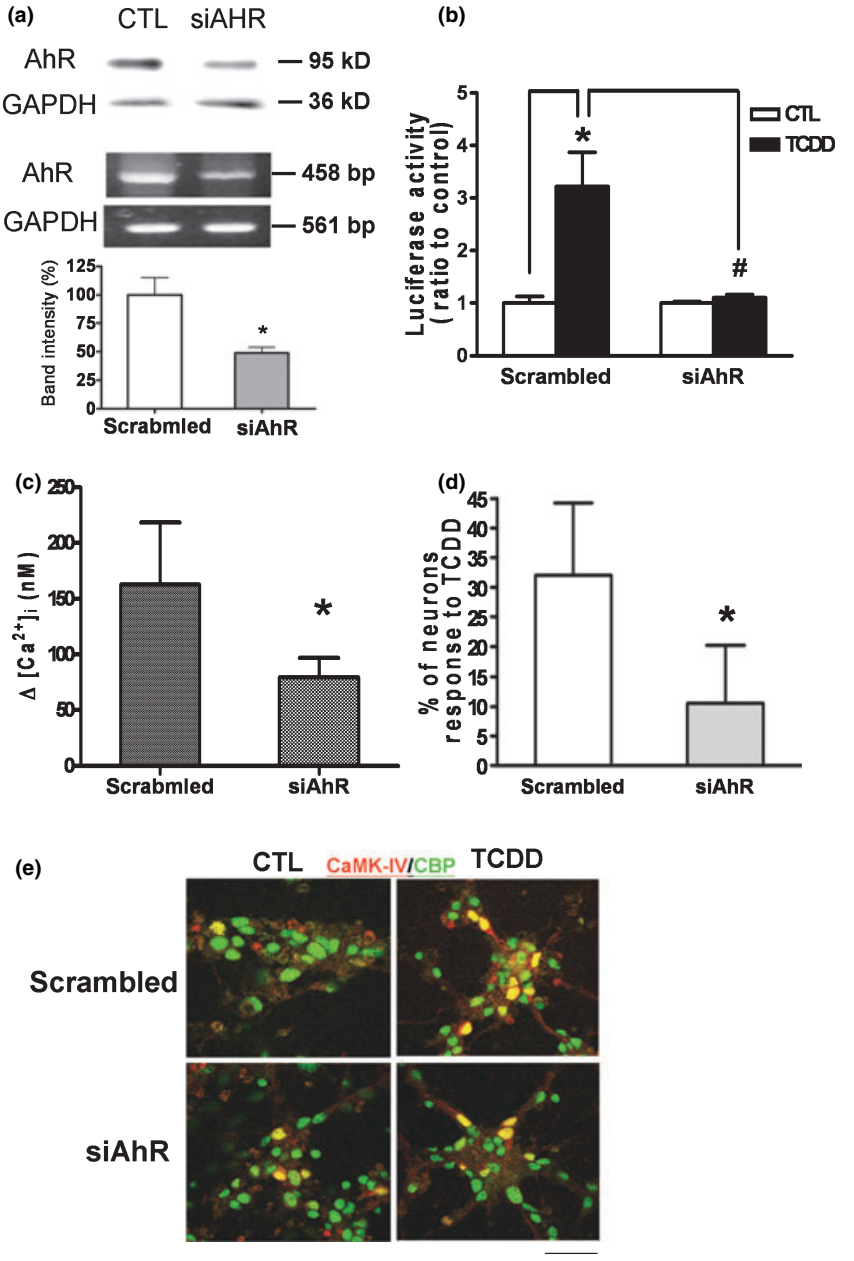

Fig. 5 Knockdown of AhR expression reduces TCDD-induced DRE-driven gene expression, calcium influx, and nuclear translocation of CaMK-IV. (a) Cortical neurons at 10 DIV were transfected with siAhR or scrambled RNA (sc) for 5 h in the lipofectamine-containing medium, and recovered in the culture medium for another 72 h. The expression of AhR and GAPDH was measured by western blotting and RT-PCR analysis. The relative band density of the AhR mRNA from the RT-PCR analysis was obtained from three batches of siAhR cell culture and were averaged and graphed. In (b and c), the siAhR-transfected cortical neurons were subjected to 20 nmol/L TCDD for the DRE-driven luciferase activity assay (b), $[Ca^{2+}]_i$ measurements by confocal microscopy (c) and fluorescent spectrophotometry (d), and fluorescent double labeling of CaMK-IV (red by Texas Red) and CBP (green by FITC) (e). (e) Shows the merged images of CaMK-IV/CBP co-localized structures in yellow. Data represent the mean ± SEM ($n = 3$). *$p < 0.05$ when compared with the respective control group. Scale bar: 50 μm.

blockers. Figure 6a and b show that TCDD-induced LDH release and decrease of MTT reduction activity were much more profound in 10 DIV than in 4 DIV neurons. In 10 DIV neurons, TCDD-reduced cell survival appeared after 48 h of treatment, and was insignificant if the concentration of TCDD was lower than 10 nmol/L. As this result was similar to the observations in AhR-mediated gene expression, we further examined if dioxin neurotoxicity in 10 DIV neurons is activity-dependent. Figure 6c shows that MK801, TTX, and KN-93 were all effective in reducing TCDD neurotoxicity, and MK801 was the more potent than another two inhibitors. Collectively, these results suggest that synaptic

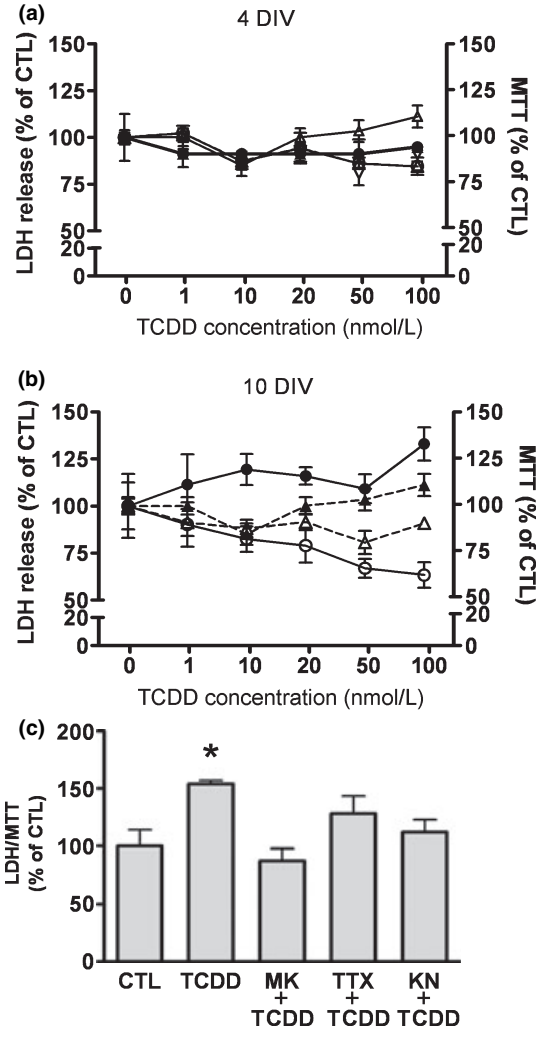

Fig. 6 TCDD reduces neuronal survival in an activity-dependent manner. Cortical neurons at 4 and 10 DIV (a and b) were treated with TCDD at 1, 10, 20, 50, and 100 nmol/L for 24 (triangle) and 48 h (circle), followed by LDH release (solid line) and MTT reduction activity (dashed line) analysis. (c) Cortical neurons at 10 DIV were treated with 20 nmol/L TCDD in the presence or absence of 10 μmol/L MK801, 1 μmol/L TTX, and 10 μmol/L KN-93, followed by LDH release and MTT reduction activity analysis. The ratio of LDH activity to MTT activity in each group represents cell death rate. Data represent the mean ± SEM ($n = 4$). *$p < 0.05$ when compared with the respective control group by unpaired *t*-test.

activity may enhance dioxin neurotoxicity in a similar fashion as it enhances AhR-mediated calcium signaling and gene expression.

Discussion

In this study, we demonstrated that AhR-mediated gene regulation in cortical neurons depends on the neuronal activity, causing developmental differences in neuronal susceptibility to dioxin insult. Inhibiting neuronal activity using TTX and MK801 resulted in a decrease of TCDD-induced dioxin-responsive gene expression, calcium influx, and neuronal death. We elucidated the underlying mechanism of action, in which plasticity-related CaMK-IV/CBP signaling plays a key role in facilitating AhR-mediated transcriptional regulation. Figure 7 shows a schematic illustration of the proposed sequence of events derived from this study for the AhR-mediated gene expression and neurotoxicity in cortical neurons. The information obtained from this study provides important information for evaluating the susceptibility of mammalian brains to environmental toxins with similar mechanism of actions.

The primary finding of our study is that the activity-dependent transcriptional regulation of dioxin-responsive gene expression depends on the developmental stage of cultured cortical neurons. Neuronal activity is known to be involved in gene expressions for neural differentiation, axonal growth, and synaptic maturation (Kim and Yang 2005). The impact of neuronal activity on AhR-mediated gene expression seems to be associated with synaptic activity rather than the early stages of neuronal development. This finding explains why other studies observed that dioxin neurotoxicity, or dioxin-altered gene expression, were more profound not only in the developing brain but also in highly plastic brain regions in adults. In fact, neuronal activity is involved in the maturation of excitatory synaptic connections and expression of synaptic proteins (Takada *et al.* 2005; Kitamura *et al.* 2007). Developmental changes of the NMDA-R subunit composition also depend on synaptic activity, in which the expression of NR1 mRNA splice variants and NR2A are up-regulated in cultured cortical neurons with increasing time in culture (Hoffmann *et al.* 2000). Our previous study also demonstrated that the neuronal susceptibility to glutamate insult is also maturation-dependent in the same neuronal culture system (Lee *et al.* 2000). Therefore, it is likely that the activity-dependent AhR-mediated gene expression and dioxin neurotoxicity is owing to the developmental changes of synaptic properties and NMDA-R activity. In addition, we found that CaMK-IV is involved in activity-dependent AhR activity and dioxin neurotoxicity. CaMK-IV plays an important role in mediating activity-dependent synaptic plasticity, such as consolidation of long-term memory and activation of plasticity-related signaling proteins (Mao *et al.* 1999; Szebenyi *et al.* 2005; Ince-Dunn *et al.* 2006). CaMK-IV activation of CBP is also required for activating cAMP-response element binding protein, a transcription factor that plays important role in adaptive plasticity and long-term potentiation (Kang *et al.* 2001; Wei *et al.* 2002). This poses the question of whether activation of CaMK-IV/CBP by dioxin results in the interference of CaMK-IV-mediated synaptic activity.

Although AhR activation in neurons seems to be activity-dependent, it is noteworthy that the action potential blocker

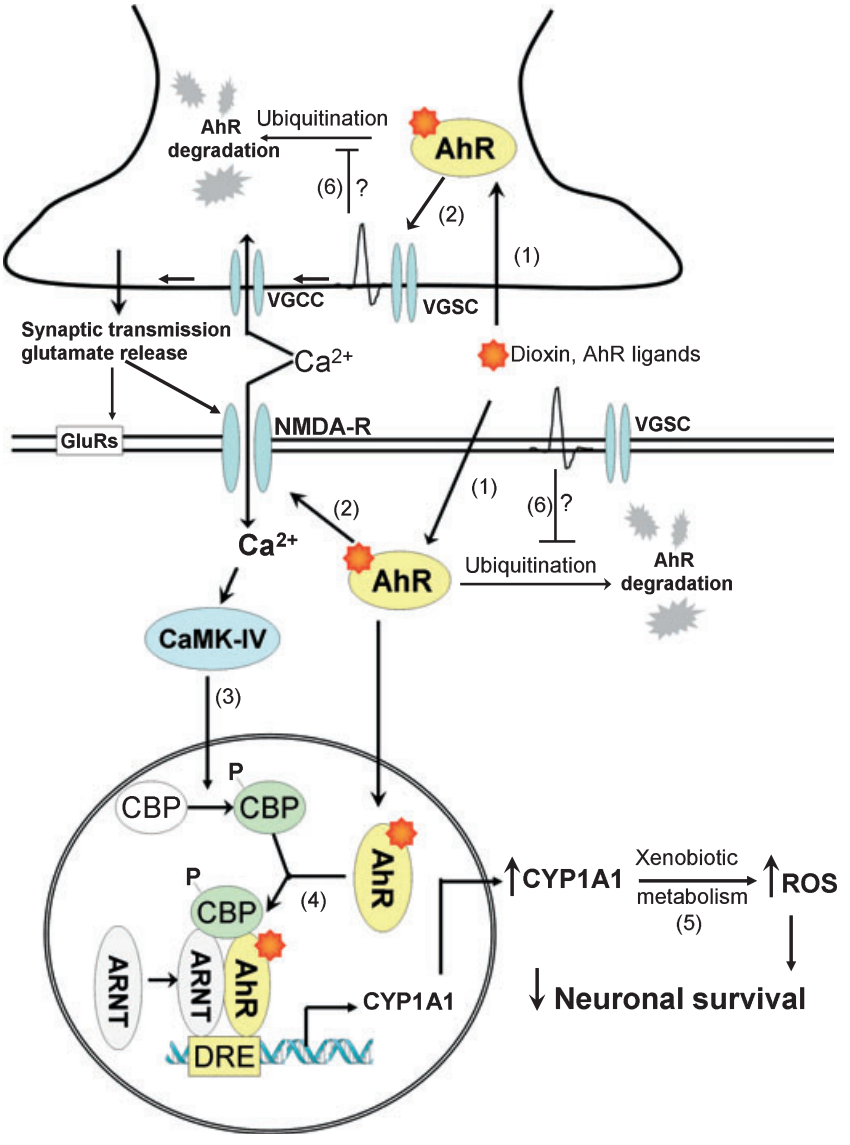

Fig. 7 Neuronal activity enhancement of AhR activities in cortical neurons – the proposed mechanism. (1) TCDD binds to AhR and induces its translocation from cytoplasm into the nucleus. (2) TCDD-bound AhR in the cytoplasm also induces calcium influx via NMDA-R and TTX-sensitive calcium entry, which is responsible for the synaptic transmission in mature neurons. TTX blocks the voltage-sensitive sodium channel (VGSC) and subsequent action potential firing, which is responsible for the voltage-gated calcium channel (VGCC) opening. (3) AhR-induced calcium influx through NMDA-R further activates CaMK-IV and induces its nuclear translocation to activate the AhR co-activator CBP by phosphorylation. This step can be enhanced by the synaptic transmission in mature neurons. (4) Activated CBP interacts with the AhR-ARNT complex to facilitate its binding to DRE on the cyp1A1 enhancer, which results in the enhancement of CYP1A1 gene expression. (5) Enhanced CYP1A1 expression gives rise to increase of ROS production during xenobiotic metabolism of TCDD, which leads to reduced neuronal survival rate. (6) The activity-dependent blockade of ubiquitination as reported by other studies might involve in the enhancement of AhR activities.

TTX, and the NMDA-R channel blocker MK801, had differential effects on the maturation-dependent CYP1A1 expression and association of AhR and CBP to the cyp1A1 enhancer induced by TCDD. MK801 could reduce CYP1A1 in both 4 and 10 DIV cortical neurons, suggesting that the NMDA-R-mediated neuronal activity is involved in AhR activity throughout the neuronal development. Interestingly, TTX only blocked TCDD-induced CYP1A1 expression in 10 DIV but not 4 DIV neurons, suggesting that the maturation-dependent AhR activity is contributed by the synaptic formation. In the ChIP assay study, MK801 had a stronger effect than TTX on reducing the association of CBP with the cyp1A1 enhancer in the ChIP assay, suggesting that the NMDA-R may contribute to the enhancement of AhR transactivation via activation of CBP. Moreover, it is interesting that TTX abolishes AhR binding to the cyp1A1 enhancer, suggesting that activation of AhR may also depend on neuronal activity. Recent studies have revealed that neuronal activity could reduce ubiquitin-proteosome activity-dependent viral immediate-early protein expression in primary neuronal cultures (Ho *et al.* 2000; Impey *et al.* 2002). As the ubiquitin-proteosome system is involved in the homeostasis of AhR, it is worth further investigating whether neuronal activity influences the stability of activated AhR via regulation of AhR degradation. A hypothesized step regarding the involvement of activity-dependent regulation of AhR ubiquitination was proposed in Figure 7.

Although the $[Ca^{2+}]_i$-elevating effect of TCDD via the NMDA-R has been demonstrated previously, this is the first report on the activity- and maturation-dependent effects of TCDD. This finding not only provides a clue for evaluating dioxin susceptibility in the brain, but also elucidates the role

of dioxin-elevated $[Ca^{2+}]_i$ in the induction of gene expression, i.e. activation of CaMK-IV. In the siAhR experiment, AhR was essential, not only for dioxin-induced calcium influx, but also for the TCDD-induced nuclear translocation of CaMK-IV (Fig. 5). As the activation of CaMK-IV also depends on the NMDA-R, this poses the question of how the AhR interplay with the NMDA-R. One possibility is that AhR knockdown might affect the expression and function of the NMDA-R, as other studies has revealed that TCDD could alter the expression of NMDA-R subunits (Everett *et al.* 1998; Cho *et al.* 2002; Zhang *et al.* 2005), but the results in these studies vary depending on the experimental systems. On the other hand, a recent study reveals a new role of AhR as a target selector of E3 ubiquitin ligase in the degradation of steroid hormone receptors (Nayyar *et al.* 2003). As the ubiquitin-proteasome system has emerged as a key regulator of synaptic development, long-term potentiation, and dendritic protein degradation (Ohtake *et al.* 2007), it remains to be resolved whether this new role of AhR could account for its crosstalk with the NMDA-R.

The homeostatic modification of synaptic structure and membrane excitability are important for both neuronal development and for synaptic plasticity functions in the adult brain, such as learning and memory and other cognitive functions (Bingol and Schuman 2006; Fonseca *et al.* 2006; Patrick 2006). Our study further reveals that the engagement of AhR in the synaptic activity-dependent calcium signaling may contribute to the susceptibility of neurons to dioxin. The elucidated mechanisms correlate well with the epidemiological studies showing that TCDD preferentially impairs brain function in the developing brains of newborns upon lactational or gestational exposure to dioxin or other AhR ligands. Therefore, from a toxicological perspective, our results provide evidence that dioxin may preferentially affect neuronal survival in developing neurons at synaptic formation stage, thereby resulting in neonatal CNS disorders related to synaptic homeostasis and stabilization. However, it is noted that TCDD could not kill the cell even at very high concentration of 100 nmol/L until 48 h treatment, which took much longer time than other neurotoxic agents such as glutamate, hydrogen peroxide, or ceramide-induced neuronal death. The reason could be because of the fact that primary induction of CYP1A1 expression by dioxin for xenobiotic metabolism is not a toxic event, but longer exposure results in over-expression of CYP1A1 and lead to excessive ROS production and in turn causes reduction of cell survival. As TCDD is a persistent environmental pollutant and cannot be well degraded by CYP1A1, it is conceivable that it may accumulate in tissues with much longer duration than other neurotoxic substances with shorter half-life. Moreover, this study implicates that AhR may interplay with the NMDA-R under the physiological condition to regulate synaptic plasticity or neuronal survival. How AhR involves in the NMDA-R function is currently under investigation.

Acknowledgements

This work serves as the doctoral thesis of C-HL. This study was supported by grants NSC92-2745-P038-005 and NSC94-2320-B038-002 (93GMP002-2) from National Science Council, and Topnotch Stroke Center grant from Ministry of Education, Taiwan. We thank Dr Chung Y. Hsu at Taipei Medical University and Dr Jang-Yen Wu at Florida Atlantic University for their generous critiques. The technical assistance from Jia-Wei Ho, Tzu-Ming Ho, and Yi-Ling Lin are appreciated.

Supplementary material

The following supplementary material is available for this article online:

Fig. S1 Characterization of primary cultured cortical neurons.

This material is available as part of the online article from http://www.blackwell-synergy.com.

Please note: Blackwell Publishing are not responsible for the content or functionality of any supplementary materials supplied by the authors. Any queries (other than missing material) should be directed to the corresponding author for the article.

References

Beischlag T. V., Wang S., Rose D. W., Torchia J., Reisz-Porszasz S., Muhammad K., Nelson W. E., Probst M. R., Rosenfeld M. G. and Hankinson O. (2002) Recruitment of the NCoA/SRC-1/p160 family of transcriptional coactivators by the aryl hydrocarbon receptor/aryl hydrocarbon receptor nuclear translocator complex. *Mol. Cell. Biol.* **22**, 4319–4333.

Bingol B. and Schuman E. M. (2006) Activity-dependent dynamics and sequestration of proteasomes in dendritic spines. *Nature* **441**, 1144–1148.

Bock K. W. and Kohle C. (2006) Ah receptor: dioxin-mediated toxic responses as hints to deregulated physiologic functions. *Biochem. Pharmacol.* **72**, 393–404.

Chang D. T. W. and Reynolds I. J. (2006) Differences in mitochondrial movement and morphology in young and mature primary cortical neurons in culture. *Neuroscience* **141**, 727–736.

Cho J., Kim Y. H., Kong J. Y., Yang C. H. and Park C. G. (2002) Protection of cultured rat cortical neurons from excitotoxicity by asarone, a major essential oil component in the rhizomes of *Acorus gramineus*. *Life Sci.* **71**, 591–599.

Dale Y. R. and Eltom S. E. (2006) Calpain mediates the dioxin-induced activation and down-regulation of the aryl hydrocarbon receptor. *Mol. Pharmacol.* **70**, 1481–1487.

Duguid I. and Sjostrom P. J. (2006) Novel presynaptic mechanisms for coincidence detection in synaptic plasticity. *Curr. Opin. Neurobiol.* **16**, 312–322.

Everett R. D., Orr A. and Preston C. M. (1998) A viral activator of gene expression functions via the ubiquitin-proteasome pathway. *EMBO J.* **17**, 7161–7169.

Fonseca R., Vabulas R. M., Hartl F. U., Bonhoeffer T. and Nagerl U. V. (2006) A balance of protein synthesis and proteasome-dependent degradation determines the maintenance of LTP. *Neuron* **52**, 239–245.

Hahn M. E. (1998) The aryl hydrocarbon receptor: a comparative perspective. *Comp. Biochem. Physiol. C Pharmacol. Toxicol. Endocrinol.* **121**, 23–53.

Hanneman W. H., Legare M. E., Barhoumi R., Burghardt R. C., Safe S. and Tiffany-Castiglioni E. (1996) Stimulation of calcium uptake in cultured rat hippocampal neurons by 2,3,7,8-tetrachlorodibenzo-p-dioxin. *Toxicology* **112**, 19–28.

Hardingham G. E., Chawla S., Cruzalegui F. H. and Bading H. (1999) Control of recruitment and transcription-activating function of CBP determines gene regulation by NMDA receptors and L-type calcium channels. *Neuron* **22**, 789–798.

Hays L. E., Carpenter C. D. and Petersen S. L. (2002) Evidence that GABAergic neurons in the preoptic area of the rat brain are targets of 2,3,7,8-tetrachlorodibenzo-p-dioxin during development. *Environ. Health Perspect.* **110**, 369–376.

Ho N., Liauw J. A., Blaeser F. *et al.* (2000) Impaired synaptic plasticity and cAMP response element-binding protein activation in Ca^{2+}/calmodulin-dependent protein kinase type IV/Gr-deficient mice. *J. Neurosci.* **20**, 6459–6472.

Hoffmann H, Gremme T, Hatt H and Gottmann K. (2000) Synaptic activity-dependent developmental regulation of NMDA receptor subunit expression in cultured neocortical neurons. *J. Neurochem.* **75**, 1590–1599.

Hood DB, Woods L, Brown L, Johnson S and Ebner FF. (2006) Gestational 2,3,7,8-tetrachlorodibenzo-p-dioxin exposure effects on sensory cortex function. *Neurotoxicology* **6**, 1032–1042.

Hu S.-C., Chrivia J. and Ghosh A. (1999) Regulation of CBP-mediated transcription by neuronal calcium signaling. *Neuron* **22**, 799–808.

Impey S., Fong A. L., Wang Y., Cardinaux J.-R., Fass D. M., Obrietan K., Wayman G. A., Storm D. R., Soderling T. R. and Goodman R. H. (2002) Phosphorylation of CBP mediates transcriptional activation by neural activity and CaM kinase IV. *Neuron* **34**, 235–244.

Ince-Dunn G., Hall B. J., Hu S.-C., Ripley B., Huganir R. L., Olson J. M., Tapscott S. J. and Ghosh A. (2006) Regulation of thalamocortical patterning and synaptic maturation by NeuroD2. *Neuron* **49**, 683–695.

Jung U., Zheng X., Yoon S.-O. and Chung A.-S. (2001) Se-Methylselenocysteine induces apoptosis mediated by reactive oxygen species in HL-60 cells. *Free Radic. Biol. Med.* **31**, 479–489.

Kang H., Sun L. D., Atkins C. M., Soderling T. R., Wilson M. A. and Tonegawa S. (2001) An important role of neural activity-dependent CaMKIV signaling in the consolidation of long-term memory. *Cell* **106**, 771–783.

Kim S. Y. and Yang J. H. (2005) Neurotoxic effects of 2,3,7,8-tetrachlorodibenzo-p-dioxin in cerebellar granule cells. *Exp. Mol. Med.* **37**, 58–64.

Kitamura C, Takahashi M, Kondoh Y, Tashiro H and Tashiro T. (2007) Identification of synaptic activity-dependent genes by exposure of cultured cortical neurons to tetrodotoxin followed by its withdrawal. *J. Neurosci. Res.* **85**, 2385–2399.

Knerr S. and Schrenk D. (2006) Carcinogenicity of 2,3,7,8-tetrachlorodibenzo-p-dioxin in experimental models. *Mol. Nutr. Food Res.* **50**, 897–907.

Kobayashi A, Numayama-Tsuruta K, Sogawa K and Fujii-Kuriyama Y. (1997) CBP/p300 functions as a possible transcriptional coactivator of Ah receptor nuclear translocator (Arnt). *J. Biochem. (Tokyo)* **122**, 703–710.

Le Ferrec E., Lagadic-Gossmann D., Rauch C., Bardiau C., Maheo K., Massiere F., Le Vee M., Guillouzo A. and Morel F. (2002) Transcriptional Induction of CYP1A1 by oltipraz in human Caco-2 cells is aryl hydrocarbon receptor- and calcium-dependent. *J. Biol. Chem.* **277**, 24780–24787.

Lee Y.-H., Fang K.-M., Yang C.-M., Hwang H.-M., Chiu C.-T. and Tsai W. (2000) Kainic acid-induced neurotrophic activities in developing cortical neurons. *J. Neurochem.* **74**, 2401–2411.

Ma Q. (2001) Induction of CYP1A1. The AhR/DRE paradigm: transcription, receptor regulation, and expanding biological roles. *Curr. Drug Metab.* **2**, 149–164.

Mao Z., Bonni A., Xia F., Nadal-Vicens M. and Greenberg M. E. (1999) Neuronal activity-dependent cell survival mediated by transcription factor MEF2. *Science* **286**, 785–790.

Marshall J., Dolan B. M., Garcia E. P., Sathe S., Tang X., Mao Z. and Blair L. A. C. (2003) Calcium channel and NMDA receptor activities differentially regulate nuclear C/EBP[β] levels to control neuronal survival. *Neuron* **39**, 625–639.

McCarthy K. D. and de Vellis J. (1980) Preparation of separate astroglial and oligodendroglial cell cultures from rat cerebral tissue. *J. Cell Biol.* **85**, 890–902.

Mimura J. and Fujii-Kuriyama Y. (2003) Functional role of AhR in the expression of toxic effects by TCDD. *Biochim. Biophy. Acta* **1619**, 263–268.

Nayyar T., Wu J. and Hood D. B. (2003) Downregulation of hippocampal NMDA receptor expression by prenatal exposure to dioxin. *Cell. Mol. Biol. (Noisy-le-grand)* **49**, 1357–1362.

Nishijo M, Kuriwaki J, Hori E, Tawara K, Nakagawa H and Nishijo H. (2007) Effects of maternal exposure to 2,3,7,8-tetrachlorodibenzo-*p*-dioxin on fetal brain growth and motor and behavioral development in offspring rats. *Toxicol. Lett.* **173**, 41–47.

Ohtake F., Baba A., Takada I. *et al.* (2007) Dioxin receptor is a ligand-dependent E3 ubiquitin ligase. *Nature* **446**, 562–566.

Patandin S., Lanting C. I., Mulder P. G., Boersma E. R., Sauer P. J. and Weisglas-Kuperus N. (1999) Effects of environmental exposure to polychlorinated biphenyls and dioxins on cognitive abilities in Dutch children at 42 months of age. *J. Pediatr.* **134**, 33–41.

Patrick G. N. (2006) Synapse formation and plasticity: recent insights from the perspective of the ubiquitin proteasome system. *Curr. Opin. Neurobiol.* **16**, 90–94.

Powers B. E., Lin T. M., Vanka A., Peterson R. E., Juraska J. M. and Schantz S. L. (2005) Tetrachlorodibenzo-p-dioxin exposure alters radial arm maze performance and hippocampal morphology in female $AhR^{+/-}$ mice. *Genes Brain Behav.* **4**, 51–59.

Rao V. R. and Finkbeiner S. (2007) NMDA and AMPA receptors: old channels, new tricks. *Trends Neurosci.* **30**, 284–291.

Rowlands J. C. and Gustafsson J. A. (1997) Aryl hydrocarbon receptor-mediated signal transduction. *Crit. Rev. Toxicol.* **27**, 109–134.

Schantz S. L, Gasior D. M, Polverejan E, McCaffrey R. J., Sweeney A. M., Humphrey H. E. B. and Gardiner J. C. (2001) Impairments of memory and learning in older adults exposed to polychlorinated biphenyls via consumption of Great Lakes fish. *Environ. Health Perspect.* **109**, 605–611.

Seegal R. F. (1996) Epidemiological and laboratory evidence of PCB-induced neurotoxicity. *Crit. Rev. Toxicol*. **26**, 709–737.

Shimada T. and Fujii-Kuriyama Y. (2004) Metabolic activation of polycyclic aromatic hydrocarbons to carcinogens by cytochromes P450 1A1 and 1B1. *Cancer Sci* **95**, 1–6.

Szebenyi G., Bollati F., Bisbal M., Sheridan S., Faas L., Wray R., Haferkamp S., Nguyen S., Caceres A. and Brady S. T. (2005) Activity-driven dendritic remodeling requires microtubule-associated protein 1A. *Curr. Biol.* **15**, 1820–1826.

Takada N, Yanagawa Y and Komatsu Y. (2005) Activity-dependent maturation of excitatory synaptic connections in solitary neuron cultures of mouse neocortex. *Eur. J. Neurosci.* **21**, 422–430.

Wei F., Qiu C., Liauw J. A., Robinson D., Ho N., Chatila T. A. and Zhuo M. (2002) Calcium calmodulin-dependent protein kinase IV is required for fear memory. *Nat. Neurosci.* **5**, 573–579.

Weiss S., Pin J.-P., Sebben M., Kemp D. E., Sladeczek F., Gabrion J. and Bockaert J. (1986) Synaptogenesis of cultured striatal neurons in serum-free medium: a morphological and biochemical study. *Proc. Natl Acad. Sci. USA* **83**, 2238–2242.

Williamson M. A., Gasiewicz T. A. and Opanashuk L. A. (2005) Aryl hydrocarbon receptorexpression and activity in cerebellar granule neuroblasts: implications for development and dioxin neurotoxicity. *Toxicol. Sci.* **83**, 340–348.

Wong P. W., Joy R. M., Albertson T. E., Schantz S. L. and Pessah I. N. (1997) Ortho-substituted 2,2′,3,5′,6-pentachlorobiphenyl (PCB 95) alters rat hippocampal ryanodine receptors and neuroplasticity in vitro: evidence for altered hippocampal function. *Neurotoxicology* **18**, 443–456.

Zhang C. X., Ofiyai H., He M., Bu X., Wen Y. and Jia W. (2005) Neuronal activity regulates viral replication of herpes simplex virus type 1 in the nervous system. *J. Neurovirol.* **11**, 256–264.

Zhao X., MacBride M. M., Peterson B. R., Pfaff D. W. and Vasudevan N. (2005) Calcium flux in neuroblastoma cells is a coupling mechanism between non-genomic and genomic modes of estrogens. *Neuroendocrinology* **81**, 174–182.

